

Inherent Adversarial Robustness of Deep Spiking Neural Networks: Effects of Discrete Input Encoding and Non-Linear Activations

Saima Sharmin¹, Nitin Rath¹, Priyadarshini Panda², and Kaushik Roy¹

¹ Purdue University

² Yale University

{ssharmin,rathi2,kaushik}@purdue.edu, priya.panda@yale.edu

Abstract. In the recent quest for trustworthy neural networks, we present Spiking Neural Network (SNN) as a potential candidate for inherent robustness against adversarial attacks. In this work, we demonstrate that accuracy degradation is less severe in SNNs than in their non-spiking counterparts for CIFAR10 and CIFAR100 datasets on deep VGG architectures. We attribute this robustness to two fundamental characteristics of SNNs and analyze their effects. First, we exhibit that input discretization introduced by the Poisson encoder improves adversarial robustness with reduced number of timesteps. Second, we quantify the amount of adversarial accuracy with increased leak rate in Leaky-Integrate-Fire (LIF) neurons. Our results suggest that SNNs trained with LIF neurons and smaller number of timesteps are more robust than the ones with IF (Integrate-Fire) neurons and larger number of timesteps. We overcome the bottleneck of creating gradient-based adversarial inputs in temporal domain by proposing a technique for crafting attacks from SNN.

Keywords: Spiking Neural Networks, Adversarial attack, Leaky-Integrate-Fire neuron, Input discretization

1 Introduction

Adversarial attack is one of the biggest challenges against the success of today's deep neural networks in mission critical applications [15], [10], [31]. The underlying concept of an adversarial attack is to purposefully modulate the input to a neural network such that it is subtle enough to remain undetectable to human eyes, yet capable of fooling the network into incorrect decisions. This malicious behavior was first demonstrated in 2013 by Szegedy *et. al.* [26] and Biggio *et. al.* [4] in the field of computer vision and malware detection, respectively. Since then, numerous defense mechanisms have been proposed to address this issue. One category of defense includes fine-tuning the network parameters like adversarial training [11], [17], network distillation [21], stochastic activation pruning [8] etc. Another category focuses on preprocessing the input before passing through the network like thermometer encoding [5], input quantization [30], [20], compression [12] etc. Unfortunately, most of these defense mechanisms have

been proved futile by many counter-attack techniques. For example, an ensemble of defenses based on “gradient-masking” collapsed under the attack proposed in [1]. Defensive distillation was broken by Carlini-Wagner method [6], [7]. Adversarial training has the tendency to overfit to the training samples and remain vulnerable to transfer attacks [27]. Hence, the threat of adversarial attack continues to persist.

In the absence of adversarial robustness in the existing state-of-the-art networks, we feel there is a need for a network with *inherent* susceptibility against adversarial attacks. In this work, we present Spiking Neural Network (SNN) as a potential candidate due to two of its fundamental characteristics:

1. SNNs operate based on discrete binary data (0/1), whereas their non-spiking counterparts, referred as Analog Neural Network (ANN), take in continuous-valued analog signals. Since SNN is a binary spike-based model, input discretization is a constituent element of the network, most commonly done by Poisson encoding.
2. SNNs employ nonlinear activation function of the biologically inspired Integrate-Fire (IF) or Leaky-Integrate-Fire (LIF) neurons, in contrast to the piecewise-linear ReLU activations used in ANNs.

Among the handful of works done in the field of SNN adversarial attacks [18], [2], most of them are restricted to either simple datasets (MNIST) or shallow networks. However, this work extends to complex datasets (CIFAR) as well as deep SNNs which can achieve comparable accuracy to the state-of-the-art ANNs [23], [22]. For robustness comparison with non-spiking networks, we analyze two different types of spiking networks: (1) converted SNN (trained by ANN-SNN conversion [23]) and (2) backpropagated SNN (an ANN-SNN converted network, further incrementally trained by surrogate gradient backpropagation [22]). We identify that converted SNNs fail to demonstrate more robustness than ANNs. Although authors in [24] show similar analysis, we explain with experiments the reason behind this discrepancy and, thereby, establish the necessary criteria for an SNN to become adversarially robust. Moreover, we propose an SNN-crafted attack generation technique, with the help of the surrogate gradient method. We summarize our contributions as follows:

- We show that the accuracy degradation due to adversarial attack in a spiking network is less than that in a non-spiking network. This behavior holds even for deep networks like VGG and complex datasets like CIFAR10 and CIFAR100. Note, the clean accuracy of both SNNs and ANNs are similar in our comparisons.
- The increased robustness of SNN is attributed to two fundamental characteristics: input discretization through Poisson encoding and non-linear activation due to LIF (or IF) neurons.
 - We investigate how adversarial accuracy changes with the number of timesteps (inference latency) used in SNN for different levels of input pre-quantization. In case of backpropagated SNNs (trained with smaller

number of timesteps), the amount of discretization and adversarial robustness increase as we reduce the number of timesteps. Pre-quantization of the analog input brings about further improvement. However, converted SNNs appear to depend only on the input pre-quantization, but invariant to the variation in the number of timesteps. Since these converted SNNs operate under larger number of timesteps [23], quantization effect is minimized by input averaging, and hence, the observed invariance.

- We demonstrate that piecewise-linear activation of ReLU in an ANN linearly propagates the adversarial perturbation throughout the network, whereas non-linear activations like LIF (or IF) neurons in an SNN leave a diminishing effect on the adversarial input from one layer to the next. Moreover, the leak factor of LIF neurons offers an extra knob for adversarial improvement in backpropagated SNNs. We perform a quantitative analysis of the effect of leak factor on the adversarial robustness of these types of SNNs.

Overall, backpropagated SNNs, trained with LIF neurons and smaller number of timesteps show more robustness, compared to the converted SNNs, which are trained with IF neurons and larger number of timesteps. Hence, two prerequisites for obtaining adversarially robust SNNs are smaller number of timesteps and LIF neurons. The training technique of SNN plays a crucial role in obtaining such a network.

- Gradient-based attack generation is a challenge in the SNN domain due to the non-continuous gradient of the neurons. With the help of the surrogate gradient technique, we propose a method to generate adversarial inputs from SNNs.

2 Background

2.1 Adversarial Attack

Given a clean image x belonging to class i and a trained neural network M , an adversarial image x_{adv} needs to meet two criteria:

1. x_{adv} is visually “similar” to x *i. e.* $|x - x_{adv}| = \epsilon$, where ϵ is a small number.
2. x_{adv} is misclassified by the neural network, *i. e.* $M(x_{adv}) \neq i$

The choice of the distance metric $|\cdot|$ depends on the method used to create x_{adv} and ϵ is a hyper-parameter. In most methods, l_2 or l_∞ norm is used to measure the similarity and the value of ϵ is limited to $\leq \frac{8}{255}$ where normalized pixel intensity $x \in [0, 1]$ and original $x \in [0, 255]$.

In this work, we construct adversarial examples using the following two methods:

Fast Gradient Sign Method (FGSM) This is one of the simplest methods for constructing adversarial examples, introduced in [11]. For a given instance x , true label y_{true} and the corresponding cost function of the network $J(x, y_{true})$,

this method aims to search for a perturbation δ such that it maximizes the cost function for the perturbed input $J(x + \delta, y_{true})$ subject to the constraint $|\delta|_\infty < \epsilon$. In closed form, the attack is formulated as,

$$x_{adv} = x + \epsilon \times \text{sign}(\nabla_x J(x, y_{true})) \quad (1)$$

Here ϵ denotes the strength of the attack.

Projected Gradient Descent (PGD) This method, proposed in [17], produces more powerful adversary. PGD is basically a *k-step* variant of FGSM computed as,

$$x_{adv}^{(k+1)} = \Pi_{x+\epsilon} \left\{ \left(x_{adv}^{(k)} + \alpha \times \text{sign}(\nabla_x (J(x_{adv}^{(k)}, y_{true}))) \right) \right\} \quad (2)$$

where $x_{adv}^{(0)} = x$ and $\alpha (\leq \epsilon)$ refers to the amount of perturbation used per iteration or step, k is the total number of iterations. $\Pi_{x+\epsilon}\{\cdot\}$ performs a projection of its operand on an ϵ -ball around x , *i. e.*, the operand is clipped between $x + \epsilon$ and $x - \epsilon$. Another variant of this method adds a random perturbation of strength ϵ to x before performing PGD operation.

Depending on the knowledge of the attacker, adversarial attacks are broadly categorized into two groups:

- **Whitebox attack:** In this category, the attacker has complete access to the target network, hence, target model parameters are used to craft the perturbation, which typically creates stronger adversary.
- **Blackbox attack:** In this method, the attacker has zero knowledge of the target network parameters. Hence, a different network and/or a different dataset is used to design the adversary.

2.2 Spiking Neural Network (SNN)

The main difference between an SNN and an ANN is the concept of time. The incoming signals as well as the intermediate node inputs/outputs in an ANN are static analog values, whereas in an SNN, they are binary spikes with a value of 0 or 1, which are also functions of time. In the input layer, a Poisson event generation process is used to convert the continuous valued analog signals into binary spike train. Suppose the input image is a 3-D matrix of dimension $h \times w \times l$ with pixel intensity in the range $[0, 1]$. At every time step of the SNN operation, a random number (from the normal distribution $\mathcal{N}(0, 1)$) is generated for each of these pixels. A spike is triggered at that time step if the corresponding pixel intensity is greater than the generated random number. This process continues for a total of T timesteps to produce a spike train for each pixel. Hence, the size of the input spike train is $T \times h \times w \times l$. For a large enough T , the timed average of the spike train will be proportional to its analog value.

Every node of the SNN is accompanied with a neuron. Among many neuron

models, the most commonly used ones are Integrate-Fire (IF) or Leaky-Integrate-Fire (LIF) neurons. The dynamics of the neuron membrane potential at time $t+1$ is described by,

$$V(t+1) = \lambda V(t) + \sum_i w_i x_i(t) \quad (3)$$

Here $\lambda = 1$ for IF neurons and < 1 for LIF neurons. w_i denotes the synaptic weight between current neuron and i -th pre-neuron. $x_i(t)$ is the input spike from the i -th pre-neuron at time t . When $V(t+1)$ reaches the threshold voltage V_{th} , an output spike is generated and the membrane potential is reset to 0, or in case of soft reset, reduced by the amount of the threshold voltage. At the output layer, inference is performed based on the cumulative membrane potential of the output neurons after the total time T has elapsed.

One of the main shortcomings of SNNs is that they are difficult to train, especially for deeper networks. Since the neurons in an SNN have discontinuous gradients, standard gradient-descent techniques do not directly apply. In this work, we use two of the supervised training algorithms [23], [22], which achieve ANN-like accuracy even for deep neural networks and on complex datasets.

ANN-SNN Conversion This training algorithm was originally outlined in [9] and subsequently improved in [23] for deep networks. Note that the algorithm is suited for training SNNs with IF neurons only. They propose a threshold-balancing technique that sequentially tunes the threshold voltage of each layer. Given a trained ANN, the rst step is to generate the input Poisson spike train for the network over the training set for a large enough time-window so that the timed average accurately describes the input. Next, the maximum value of $\sum_i w_i x_i$ (term 2 in Eq. 3) received by layer 1 is recorded over the entire time range for several minibatch of training data. This is referred as the maximum activation for layer 1. The threshold value of layer 1 neuron is replaced by this maximum activation keeping the synaptic weights unchanged. Such threshold tuning operation ensures that the IF neuron activity precisely mimics the ReLU function in the corresponding ANN. After balancing layer 1 threshold, the method is continued for all subsequent layers sequentially.

Conversion & Surrogate-Gradient Backpropagation In order to take advantage of the standard backpropagation-based optimization procedures, authors in [3], [32], [29] introduced the surrogate gradient technique. The input-output characteristics of an LIF (or IF) neuron is a step function, the gradient of which is discontinuous at the threshold point (Fig. 1). In surrogate gradient technique, the gradient is approximated by pseudo-derivative like linear or exponential function. Authors in [22] proposed a novel approximation function for these gradients by utilizing the spike time information in the derivative. The gradient at timestep t is computed as follows:

$$\frac{\partial o^t}{\partial u^t} = \alpha e^{-\beta \Delta t} \quad (4)$$

Here o^t is the output spike at time t , u^t is the membrane potential at t , Δt is the difference between current timestep and the last timestep post-neuron generated a spike. α and β are hyperparameters. Once the neuron gradients are approximated, back-propagation through time (BPTT) [28] is performed using the chain rule of derivatives. In BPTT, the network is unrolled over all timesteps. The final output is computed as the cumulation of outputs at every timestep and eventually, loss is defined on the summed output. During backward propagation of the loss, the gradients are accumulated over time and used in gradient-descent optimization. Authors in [22] proposed a hybrid training procedure in which the surrogate gradient training is preceded by an ANN-SNN conversion to initialize the weights and thresholds of the network. The advantage of this method over ANN-SNN conversion is twofold: one can train a network with both IF and LIF neurons and the number of timesteps required for training is reduced by a factor of 10 without losing accuracy.

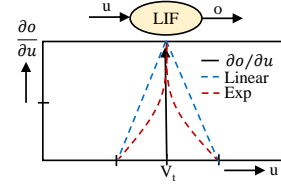


Fig. 1. Surrogate gradient approximation of an LIF neuron.

3 Experiments

3.1 Dataset and Models

We conduct our experiments on VGG5 for CIFAR10 dataset and VGG11 for CIFAR100. The network topology for VGG5 consists of conv3,64-avgpool-conv3,128 ($\times 2$)-avgpool-fc1024 ($\times 2$)-fc10. Here conv3,64 refers to a convolutional layer with 64 output filters and 3×3 kernel size. fc1024 is a fully-connected layer with 1024 output neurons. VGG11 contains 11 weight layers corresponding to the configuration A in [25] with maxpool layers replaced by average pooling. The neurons (in both ANN and SNN) contain no bias terms, since they have an indirect effect on the threshold voltage and hence, on the convergence of SNN training. The absence of bias eliminates the use of batch normalization [13] as a regularizer. Instead, a dropout layer is used after every ReLU (except for those which are followed by a pooling layer).

3.2 Training Procedure

The aim of our experiment is to compare adversarial attack on 3 networks: 1) ANN, 2) SNN trained by ANN-SNN conversion and 3) SNN trained by back-propagation, with initial conversion. These networks will be referred as ANN, SNN-conv and SNN-BP, respectively from this point onward.

For both CIFAR10 and CIFAR100 datasets, we follow the data augmentation techniques in [16]: 4 pixels are padded on each side, and a 32×32 crop is randomly sampled from the padded image or its horizontal ip. Testing is performed on the original 32×32 images. Both training and testing data are normalized to $[0, 1]$ before using. For training the ANNs, we use cross-entropy loss with

stochastic gradient descent optimization (weight decay=0.0001, mometum=0.9). VGG5 is trained for a total of 200 epochs, with an initial learning rate of 0.1, which is divided by 10 at 100-th and 150-th epoch. VGG11 with CIFAR100 is trained for 250 epochs with similar learning schedule. During training SNN-conv networks, a total of 2500 timesteps are used for both VGG5 and VGG11 architectures. SNN-BP networks are trained for 15 epochs with cross-entropy loss and adam [14] optimizer (weight decay=0.0005). Initial learning rate is 0.0001, which is halved every 5 epochs. A total of 175 timesteps is used for VGG5 and 200 timesteps for VGG11. Training is performed with either linear surrogate gradient approximation [3] or spike time dependent approximation [22] with $\alpha = 0.3$, $\beta=0.01$ (in Eq. 4). Both techniques yield approximately similar results. Leak factor λ is kept at 0.99 in all cases, except in the analysis for the leak effect.

In order to analyze the effect of input quantization (with varying number of timesteps) and leak factors, only VGG5 networks with CIFAR10 dataset is used. The baseline clean accuracy of all of these trained networks are summarized in Table 1.

Table 1. A summary of the baseline clean accuracy of ANN, SNN-conv and SNN-BP networks. T is the total number of timesteps and λ is the leak factor for SNN-BP

	ANN	SNN-conv	SNN-BP
VGG5(CIFAR10)	90%	89.9%	89.3%
VGG11(CIFAR100)	67.1%	66.8%	64.4%
4-bit input quantization (T timesteps) [$\lambda = 0.99$ for SNN-BP]			
VGG5(CIFAR10)	89.8%	89.55% (T=300) 89.57%(T=2000)	87.5% (T=50) 88.9%(T=150)
2-bit input quantization (T timesteps) [$\lambda = 0.99$ for SNN-BP]			
VGG5(CIFAR10)	85.7%	85.13% (T=300) 85.22%(T=2000)	84.1% (T=50) 84.9%(T=150)
Leak factor, λ (T = 175 timesteps)			
VGG5(CIFAR10)	—	—	87.9% ($\lambda = 1$) 87.6% ($\lambda = 0.98$) 85.9% ($\lambda = 0.95$)

3.3 Adversarial Input Generation Methodology

In order to perform whitebox and blackbox attacks, we train two separate and independently initialized models for each of the 3 networks (ANN, SNN-conv, SNN-BP). The ANN-crafted FGSM and PGD attacks are generated using the standard techniques described in Eq. 1 and 2, respectively. For FGSM and PGD, we use non-targeted attack with $\epsilon = 8/255$. PGD attacks are performed with

iteration steps $k = 7$ and per-step perturbation $\alpha = 2/255$. In order to obtain SNN-crafted attacks, we outline a surrogate-gradient based FGSM (and PGD) technique. In SNN, analog input X is converted into poisson spike train X_{spike} which is fed into the 1st convolutional layer. If X_{rate} is the timed average of X_{spike} , the membrane potential of the 1st convolutional layer X_{conv1} can be approximated as

$$X_{conv1} \approx \text{Conv}(X_{rate}, W_{conv1}) \quad (5)$$

W_{conv1} is the weight of the 1st convolutional layer. From this equation, the sign of the gradient of the network loss function J w.r.t. X_{rate} or X is described by (detailed derivation is provided in *appendix*),

$$\text{sign}\left(\frac{\partial J}{\partial X}\right) \approx \text{sign}\left(\frac{\partial J}{\partial X_{rate}}\right) = \text{sign}\left(\text{Conv}\left(\frac{\partial J}{\partial X_{conv1}}, W_{conv1}^{180rotated}\right)\right) \quad (6)$$

Surrogate gradient technique is used to obtain $\frac{\partial J}{\partial X_{conv1}}$ from SNN, which is plugged into Eq. 6 to calculate the sign of the gradient of loss w.r.t. input. This sign matrix is later used to compute X_{adv} according to standard FGSM or PGD method. The algorithm is summarized in 1.

Algorithm 1 SNN-crafted X_{adv} : *FGSM*

Require: Input (X, y_{true}) , Trained SNN (N) with loss function J .

Ensure: $\frac{\partial J}{\partial X_{conv1}} \leftarrow 0$

for timestep t in total time T **do**

forward: Loss $J(X, y_{true})$

backward : Accumulate gradient $\frac{\partial J}{\partial X_{conv1}} + = X_{conv1}.grad$

end for

post-processing: $\text{sign}(\frac{\partial J}{\partial X}) = \text{sign}\left(\text{Conv}\left(\frac{\partial J}{\partial X_{conv1}}, W_{conv1}^{180rotated}\right)\right)$

SNN-crafted adversary: $X_{adv}^{SNN} = X + \epsilon \times \text{sign}(\frac{\partial J}{\partial X})$

4 Results

4.1 ANN vs SNN

Table 2 summarizes our results for CIFAR10 (VGG5 network) and CIFAR100 (VGG11 network) datasets in whitebox and blackbox settings. Since ANN and SNN have different operating dynamics as well as training mechanisms, the test accuracy for a given input sample varies from one another, even for identical network architectures. Hence, making comparison between the absolute values of adversarial accuracy is subject to biased conclusions. We use “adversarial loss” as a measure of the adversarial robustness of the networks, which is calculated as the difference between the test accuracy of the individual network with clean inputs, x_{clean} and corresponding adversarial inputs, x_{adv} . Say, a network M makes $p_{clean}\%$ and $p_{adv}\%$ correct predictions for inputs x_{clean} and x_{adv} , respectively.

According to our definition, adversarial loss amounts to $p_{clean}\% - p_{adv}\%$, which can be interpreted as the amount of degradation of the network’s accuracy due to adversarial attacks. Smaller value of this degradation implies more robust network. From Table 2, it is evident that SNN-BP networks exhibit the least

Table 2. A comparison of the adversarial loss (= clean test accuracy (%) - adversarial test accuracy (%)) among ANN, SNN-conv and SNN-BP networks. Smallest value of the loss for each attack case is marked in *orange text*. FGSM loss is calculated at $\epsilon = 8/255$. For PGD, $\epsilon = 8/255$, α (per-step perturbation) = $2/255$, k (number of steps) = 7. The blackbox attacks are generated from a separately trained ANN of the same network topology as the target model but different initialization

		Whitebox				Blackbox			
		ANN	SNN-conv	SNN-BP	Δ^\dagger	ANN	SNN-conv	SNN-BP	Δ^\dagger
CIFAR10									
VGG5	FGSM	77.8%	80.9%	72.9%	4.9%	69.9%	69.4%	66.5%	3.4%
	PGD	86.4%	86.9%	84.1%	2.3%	83.5%	77%	78.2%	5.3%
CIFAR100									
VGG11	FGSM	50%	56.3%	48.8%	1.2%	45.8%	45.2%	42.9%	2.9%
	PGD	58.6%	62.7%	58%	0.6%	51.4%	50.9%	47.9%	3.5%

$^\dagger\Delta$ = Adversarial loss (ANN) - Adversarial loss (SNN-BP)

amount of degradation (*orange text*) in most attack cases, irrespective of the dataset, network size or attack generation method. We also compute how much lower the loss is for SNN-BP, compared to the corresponding ANN model and show it in a separate column as Δ . The value of Δ ranges between 0.6% and 5.3%. However, the adversarial loss of SNN-conv and ANN are almost identical in most cases. Hence, we conclude that SNN-BP is inherently more robust compared to their non-spiking counterpart as well as SNN-conv networks. Note that here blackbox attacks are crafted from ANNs of the same network architecture but different initialization.

In the next two subsections, we explain two characteristics of SNNs contributing towards robustness, as well as the reason for SNN-conv not being able to show similar robustness.

Effect of input quantization and number of timesteps The main idea behind non-linear input pre-processing as a defense is to discretize continuous-valued input signals so that the network becomes non-transparent to adversarial perturbations, as long as they lie within the discretization bin. SNN is a binary

spike-based network, which demands encoding any analog valued input signal into binary spike train, and hence, we believe it has the inherent robustness. In our SNN models, we employ Poisson rate encoding, where the output spike rate is proportional to the input pixel intensity. However, the amount of discretization introduced by the Poisson encoder varies with the number of timesteps used. Hence, the adversarial loss of the network can be controlled by varying the number of timesteps as long as the clean accuracy remains within reasonable limit. This effect can be further enhanced by quantizing the analog input before feeding into the Poisson encoder. In Fig. 2 (a), we demonstrate the FGSM ad-

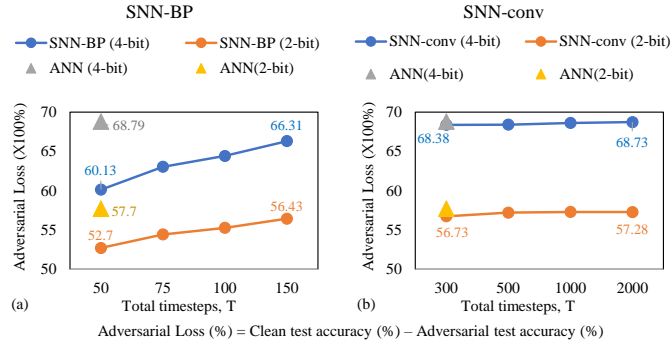


Fig. 2. Adversarial loss (%) versus total number of timesteps (T) plot with 4-bit (*blue*) and 2-bit (*orange*) input quantization for (a) SNN-BP and (b) SNN-conv networks. SNN-BP adversarial loss changes drastically with decreased number of timesteps, whereas SNN-conv is insensitive to it. In both cases, the adversary is generated from FGSM attacks ($\epsilon = 8/255$) in blackbox (ANN-crafted) condition

versarial loss of an SNN-BP network (VGG5) trained for 50, 75, 100 and 150 timesteps with CIFAR10 dataset. As number of timesteps drop from 150 to 50, loss reduces by $\sim 6\%$ (*blue line*) for 4-bit input quantization. Note that clean accuracy drops by only 1.4% within this range, from 88.9% (150 timesteps) to 87.5% (50 timesteps), as showed in Table 1. Additional reduction of the number of timesteps leads to larger degradation of clean accuracy. The adversarial loss for corresponding ANN (with 4-bit input quantization) is showed in *gray triangle* in the same plot for comparison. Additional $\sim 10\%$ decrease in adversarial loss is obtained by pre-quantizing the analog inputs to 2-bits (*orange line*) and it follows the same trend with number of timesteps. Thus varying the number of timesteps introduces an extra knob for controlling the level of discretization in SNN-BP in addition to the input pre-quantizations. In contrast, in Fig. 2(b), similar experiments performed on SNN-conv network demonstrate little decrease in adversarial loss with number of timesteps. Only pre-quantization of input signal causes a drop of adversarial loss from $\sim 68\%$ to $\sim 57\%$. Note that the range of the number of timesteps used for SNN-conv (300 to 2000) is much higher than SNN-BP, because converted networks have higher inference latency. The reason behind the invariance of SNN-conv towards the number of timesteps is explained

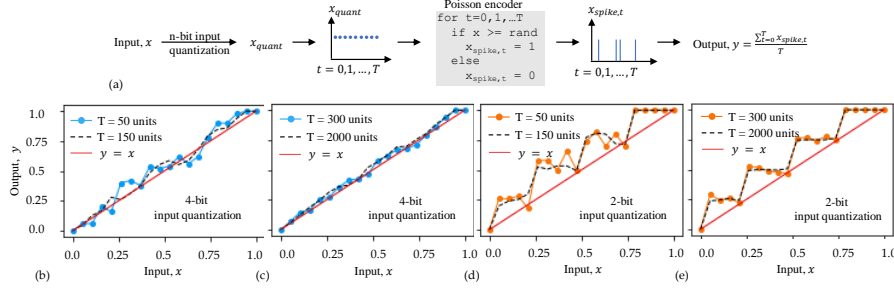


Fig. 3. The input-output characteristics of Poisson encoder to demonstrate the effect of the total number of timesteps T used to generate the spike train with different levels of pre-quantization of the analog input. When T is in the low value (between 50 to 150) regime (subplots (b) and (d)), the amount of quantization significantly changes for varying the number of timesteps (*solid dotted and dashed lines*). But in the high value regime of T (plots (c) and (e)), *solid dotted and dashed lines* almost coincide due to the averaging effect. The flow of data from output y to input x is showed in the schematic in (a)

in Fig. 3. We plot the input-output characteristics of the Poisson-encoder for 4 cases: (b) 4-bit input quantization with smaller number of timesteps (50 and 150), (c) 4-bit quantization, larger number of timesteps (300 and 2000) and their 2-bit counterparts in (d) and (e), respectively. It is evident from (c) and (e) that larger number of timesteps introduce more of an averaging effect, than quantization, and hence, varying the number of timesteps has negligible effect on the transfer plots (*solid dotted and dashed lines coincide*), which is not true for (b) and (d). Due to this averaging effect, Poisson output y for SNN-conv tends to follow the trajectory of x_{quant} (quantized ANN input), leading to comparable adversarial loss to the corresponding ANN over the entire range of timesteps in Fig. 2 (b). Note that, in these plots input x refers to the analog input signal, whereas output y is the timed average of the spike train (as showed in the schematic in Fig. 3 (a)).

Effect of LIF (or IF) neurons and the leak factor Another major contributing factor towards SNN robustness is their highly nonlinear neuron activations (Integrate-Fire or Leaky-Integrate-Fire), whereas ANNs use mostly piecewise linear activations like ReLU. In order to explain the effect of this nonlinearity, we perform a proof of concept experiment. We feed a clean and corresponding adversarial input to a ReLU and an LIF neuron ($\lambda = 0.99$ in Eq. 3). Both of the inputs are 32×32 images with pixel intensity normalized to $[0, 1]$. Row 1, 2 and 3 in Fig. 4 present the clean image, corresponding adversarial image and their absolute difference (amount of perturbation), respectively. Note, the outputs of the LIF neurons are binary at each timestep, hence, we take an average over the entire time-window to obtain corresponding pixel intensity. ReLU passes both clean and adversarial inputs without any transformation, hence the l_2 -norm of the perturbation is same at the input and ReLU output (bottom table of the fig-

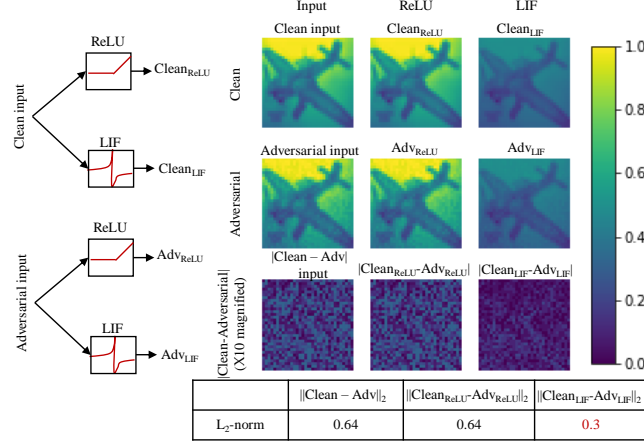


Fig. 4. The input and output of ReLU and LIF neurons are demonstrated for each of clean and adversarial image. Column 1 shows clean image, adversarial image and the absolute value of the adversarial perturbation before passing through the neurons. Column 2 and 3 depict the corresponding images after passing through a ReLU and an LIF, respectively. The bottom table contains the l_2 -norm of the perturbation at the input, ReLU output and LIF output

ure). However, the non-linear transformation in LIF reduces the perturbation of 0.6 at input layer to 0.3 at its output. Basically, the output images of LIF (column 3) neurons is a low pixel version of the input images, due to the translation of continuous analog values into a binary spike representation, which is inherently sparse. This behavior helps diminish the propagation of adversarial perturbation through the network. IF neurons also demonstrate this non-linear transformation.

However, the quantization effect is minimized due to their operation over longer time-window (as explained in the previous section). Unlike SNN-conv, SNN-BP networks can be trained with LIF neurons. The leak factor in an LIF neuron provides an extra knob to manipulate the adversarial robustness of these networks. In order to investigate the effect of leak on the amount of robustness, we develop a simple expression relating the leak factor with neuron spike rate in an LIF neuron. In this case, the membrane potential V_t at timestep t is updated according to the following equation:

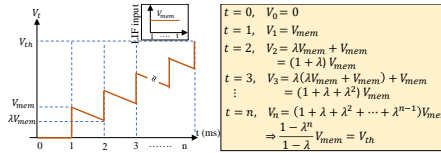


Fig. 5. Output of an LIF neuron at timestep t , given a constant input voltage.

$$V_t = \lambda V_{t-1} + V_{input,t} \quad (7)$$

given the membrane potential has not reached threshold yet, and hence, reset signal = 0. Here, λ (< 1) is the leak factor and $V_{input,t}$ is the input to the neuron at timestep t . Let us consider the scenario, where a constant voltage V_{mem} is fed into the neuron at every timestep and the membrane potential reaches the threshold voltage V_{th} after n timesteps. As explained in Fig. 5, membrane potential follows a geometric progression with time. After replacing $\frac{V_{th}}{V_{mem}}$ with a constant r , we obtain the following relation between the rate of spike ($1/n$) and leak factor (λ):

$$\text{Spike rate, } \frac{1}{n} = \frac{\log \lambda}{\log[r\lambda - (r-1)]}, \lambda < 1 \quad (8)$$

In Fig. 6(a), we plot the spike rate as a function of leak factor λ for different values of V_{mem} according to Eq. 8, where λ is varied from 0.9999 to 0.75. In every case, spike rate decreases (*i. e.* sparsity and hence, robustness increases) with increased amount of leak (smaller λ). The plot in Fig. 6(b) justifies this idea where we show the adversarial loss of an SNN-BP network (VGG5 with CIFAR10) trained with different values of leak. For both FGSM and PGD attacks, adversarial loss decreases by 6 ~ 8% as λ is decreased to 0.95. In addition to sparsity, leak makes the membrane potential (in turn, the output spike rate) dependent on the temporal information of the incoming spike train [19]. Therefore, for a given input, while the IF neuron produces a deterministic spike pattern, the input-output spike mapping is non-deterministic in an LIF neuron. This effect gets enhanced with increased leak. We assume that this phenomenon is also responsible to some extent for the increased robustness of backpropagated SNNs with increased leak. It is worth mentioning here that Eq. 8 holds when input to the neuron remains unchanged with the leak factor. In our experiments, we train SNN-BP with different values of λ starting from the same initialized ANN-SNN converted network. Hence, the parameters of SNN-BP trained with different leak

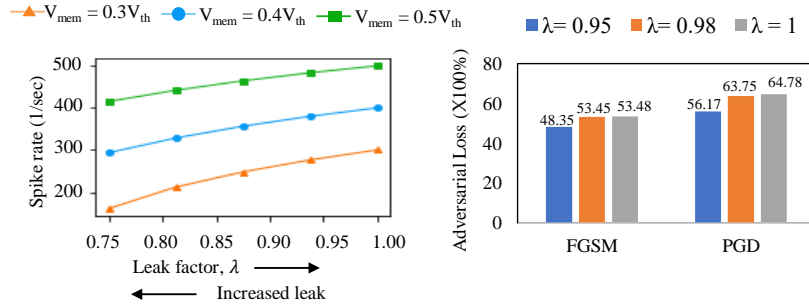


Fig. 6. (a) Spike rate versus leak factor λ for different values of $\frac{V_{mem}}{V_{th}}$. Smaller value of λ corresponds to more leak. (b) A bar plot showing the comparison of FGSM ($\epsilon = 8/255$) adversarial loss for a VGG5 SNN-BP network trained on CIFAR10 for different values of λ . These are blackbox attacks crafted from a VGG5 ANN model

factors do not vary much from one another. Therefore, the assumption in the equation applies to our results.

4.2 ANN-Crafted vs SNN-Crafted Attack

Lastly, we propose an attack-crafting technique from SNN with the aid of the surrogate gradient calculation. The details of the method is explained in Sec. 3.3. Table 3 summarizes a comparison between ANN-crafted and SNN-crafted (our proposed technique) attacks. Note, these are blackbox attacks, *i. e.*, we train two separate and independently initialized models for each of the 3 networks (ANN, SNN-conv, SNN-BP). One of them is used as the source (*marked as ANN-I, SNN-conv-I etc.*) and the other ones as target in the blackbox scenario. It is clear that SNN-BP adversarial loss is the smallest for both SNN-crafted and ANN-crafted inputs. Moreover, let us analyze row 1 of Table 3 for FGSM. When ANN-II is attacked by an ANN-I, the loss is 69.9%, whereas, if attacked by an SNN-conv-I (or SNN-BP-I), the loss is only 56% (or 57.5%). Hence, these results suggest that ANN-crafted attacks are stronger than the corresponding SNN counterparts.

5 Conclusions

The current defense mechanisms in ANNs are incapable of preventing a range of adversarial attacks. In this work, we show that SNNs are inherently resilient to adversarial attacks due to the discrete nature of input encoding and non-linear activation functions of LIF (or IF) neurons. The resiliency can be further improved by reducing the number of timesteps in the input-spike generation process and increasing the amount of leak of the LIF neurons. Note, the SNNs trained using ANN-SNN conversion technique (with IF neurons) require larger number of timesteps for inference than the corresponding SNNs trained with spike-based backpropagation (with LIF neuron). Hence, the latter training technique leads to more robust SNNs. We demonstrate the robustness of deep VGG networks on CIFAR datasets by comparing ANNs, converted SNNs, and backpropagated SNNs. We also propose a method to generate gradient-based attacks from SNNs by using the surrogate gradients.

Table 3. A comparison of ANN-crafted *versus* SNN-crafted attacks. ANN-I and ANN-II are two separately trained VGG5 networks with different initializations. The same is true for SNN-conv and SNN-BP.

	FGSM			PGD		
	ANN-I	SNN-conv-I	SNN-BP-I	ANN-I	SNN-conv-I	SNN-BP-I
ANN-II	69.9%	56%	57.5%	83.5%	56.5%	74.4%
SNN-conv-II	69.1%	55.6%	57.3%	77.0%	56.2%	74.3%
SNN-BP-II	66.5%	49.1%	55%	78.2%	44.3%	70.9%

Acknowledgement

The work was supported in part by, Center for Brain-inspired Computing (C-BRIC), a DARPA sponsored JUMP center, Semiconductor Research Corporation, National Science Foundation, Intel Corporation, the DoD Vannevar Bush Fellowship and U.S. Army Research Laboratory.

References

1. Athalye, A., Carlini, N., Wagner, D.: Obfuscated gradients give a false sense of security: Circumventing defenses to adversarial examples. In: ICML. arXiv:1802.00420 (2018)
2. Bagheri, A., Simeone, O., Rajendran, B.: Adversarial training for probabilistic spiking neural networks. In: 2018 IEEE 19th International Workshop on Signal Processing Advances in Wireless Communications (SPAWC). arXiv:1802.08567v2 (2018)
3. Bellec, G., Salaj, D., Subramoney, A., Legenstein, R., Maass, W.: Long short-term memory and learning-to-learn in networks of spiking neurons. In: Advances in Neural Information Processing Systems. pp. 787–797 (2018)
4. Biggio, B., Corona, I., Maiorca, D., Nelson, B., Srndic, N., Laskov, P., Giacinto, G., Roli, F.: Evasion attacks against machine learning at test time. ECML PKDD, part III pp. 387–402 (2013), springer
5. Buckman, J., Roy, A., Raffel, C., Goodfellow, I.: Thermometer encoding: One hot way to resist adversarial examples. In: ICLR (2018)
6. Carlini, N., Wagner, D.: Defensive distillation is not robust to adversarial examples (2016), arXiv:1607.04311
7. Carlini, N., Wagner, D.: Towards evaluating the robustness of neural networks. In: Security and Privacy (SP), 2017 IEEE Symposium on. pp. 39–57. arXiv:1608.04644 (2017)
8. Dhillon, G.S., Azizzadenesheli, K., Lipton, Z.C., Bernstein, J., Kossai, J., Khanna, A., Anandkumar, A.: Stochastic activation pruning for robust adversarial defense. In: ICLR. arXiv:1803.01442 (2018)
9. Diehl, P.U., Neil, D., Binas, J., Cook, M., Liu, S.C., Pfeifer, M.: Fast-classifying, high-accuracy spiking deep networks through weight and threshold balancing. In: 2015 International Joint Conference on Neural Networks (IJCNN). pp. 1–8 (2015)
10. Eykholt, K., Evtimov, I., Fernandes, E., Li, B., Rahmati, A., Xiao, C., Prakash, A., Kohno, T., Song, D.: Robust physical world attacks on deep learning visual classifications. In: CVPR (2018), arXiv:1707.08945v5
11. Goodfellow, I.J., Shlens, J., Szegedy, C.: Explaining and harnessing adversarial examples. In: ICLR. arXiv:1412.6572 (2015)
12. Guo, C., Rana, M., Cisse, M., van der Maaten, L.: Countering adversarial images using input transformations (2018)
13. Ioffe, S., Szegedy, C.: Batch normalization: Accelerating deep network training by reducing internal covariate shift. In: ICML. pp. 448–456 (2015)
14. Kingma, D.P., Ba, J.L.: Adam: A method for stochastic optimization. In: ICLR (2014), arXiv:1412.6980v9
15. Kurakin, A., Goodfellow, I., Bengio, S.: Adversarial examples in the physical world. In: ICLR (2017), arXiv:1607.02533v4
16. Lee, C.Y., Xie, S., Gallagher, P., Zhang, Z., Tu, Z.: Deeply-Supervised nets (2014)

17. Madry, A., Makelov, A., Schmidt, L., Tsipras, D., Vladu, A.: Towards deep learning models resistant to adversarial attacks. In: ICLR. arXiv:1706.06083 (2018)
18. Marchisio, A., Nanfa, G., Khalid, F., Hanif, M.A., Martina, M., Shaque, M.: SNN under attack: are spiking deep belief networks vulnerable to adversarial examples? (2019)
19. Olin-Ammentorp, W., Beckmann, K., Schuman, C.D., Plank, J.S., Cady, N.C.: Stochasticity and robustness in spiking neural networks (2019)
20. Panda, P., Chakraborty, I., Roy, K.: Discretization based solutions for secure machine learning against adversarial attacks. *IEEE Access* **7**, 70157–70168 (2019)
21. Papernot, N., McDaniel, P., Wu, X., Jha, S., Swami, A.: Distillation as a defense to adversarial perturbations against deep neural networks. In: Security and Privacy (SP), 2016 IEEE Symposium on. pp. 582–597 (2016)
22. Rath, N., Srinivasan, G., Panda, P., Roy, K.: Enabling deep spiking neural networks with hybrid conversion and spike timing dependent backpropagation. In: ICLR (2020), to appear
23. Sengupta, A., Ye, Y., Wang, R., Liu, C., Roy, K.: Going deeper in spiking neural networks: VGG and residual architectures. *Frontiers in neuroscience* **13**:95 (2019)
24. Sharmin, S., Panda, P., Sarwar, S.S., Lee, C., Ponghiran, W., Roy, K.: A comprehensive analysis on adversarial robustness of spiking neural networks. In: 2019 International Joint Conference on Neural Networks (IJCNN). arXiv:1905.02704v1 (2019)
25. Simonyan, K., Zisserman, A.: Very deep convolutional networks for large-scale image recognition. In: ICLR. arXiv:1409.1556 (2015)
26. Szegedy, C., Zaremba, W., Sutskever, I., Bruna, J., Erhan, D., I. Goodfellow, Fergus, R.: Intriguing properties of neural networks. In: ICLR. arXiv:1312.6199v4 (2014)
27. Tramèr, F., Kurakin, A., Papernot, N., Goodfellow, I., Boneh, D., McDaniel, P.: Ensemble adversarial training: Attacks and defenses. In: ICLR (2018), arXiv:1705.07204v4
28. Werbos, P.J.: Backpropagation through time: what it does and how to do it. *Proceedings of the IEEE* **78**(10), 1550–1560 (1990)
29. Wu, Y., Deng, L., Li, G., Zhu, J., Shi, L.: Spatio-temporal backpropagation for training high-performance spiking neural networks. *Frontiers in Neuroscience* **12** (2018)
30. Xu, W., Evans, D., Qi, Y.: Feature squeezing: Detecting adversarial examples in deep neural networks. In: Network and Distributed Systems Security Symposium (NDSS). arXiv:1704.01155 (2018)
31. Xu, W., Qi, Y., Evans, D.: Automatically evading classifiers. In: Network and Distributed Systems Security Symposium (NDSS) (2016)
32. Zenke, F., Ganguli, S.: Superspike: Supervised learning in multilayer spiking neural networks. *Neural computation* **30**(6), 1514–1541 (2018)